Spatially Controlled Fabrication of Nanoporous Block Copolymers

Mingqi Li,[†] Katsuji Douki,[†,‡] Ken Goto,[†,§] Xuefa Li,[†,∥] Christopher Coenjarts,[†] Detlef M. Smilgies,[⊥] and Christopher K. Ober*[,†]

Department of Materials Science and Engineering and Cornell High Energy Synchrotron Source (CHESS), Wilson Laboratory, Cornell University, Ithaca, NY 14853

Received April 22, 2004. Revised Manuscript Received July 21, 2004

A light-driven process for fabrication of spatially controlled nanoporous polymer films was demonstrated with a new diblock copolymer/small molecule additive system. Poly(α-methylstyrene-*b*-4-hydroxystyrene) was designed and synthesized with one block functioning as a high-resolution negative-tone photoresist and the second block being selectively removable. With a straightforward spin-coating process, a perpendicular cylindrical orientation of the removable block α-methylstyrene microdomain was induced over a wide range of film thicknesses on different substrates. Uniform nanometer-sized pores in submicron-sized photopatterns can be generated by merger of "top down" photolithographic imaging with a subsequent selective removal of a "bottom up" self-assembled nanostructure.

Introduction

As structural dimensions for nanotechnology are pushed to ever-smaller limits, the controlled fabrication of nanometer-sized structures is desirable for use in many applications.[1] Due to the simplicity, elegance, and high-yield of block copolymer fabrication approaches, they have been actively employed to fabricate nanoreactors,[2−5] nanoporous matrixes,[6−11] and functional nanorelief objects,[12,13] as well as templates for subsequent large-area high-resolution nanolithography[8,14,15] and nanoreplication.[6,16] In all of these applications, nanoporous block copolymers have been one of the most actively studied areas due to their potential application as photonic band gap materials,[17] molecular sieves,[18] or templates for magnetic storage structures.[19,20] Ever since Nakahama and co-workers[21] made the first attempt to form a monolithic nanoporous polymer thin film with a siloxane-functionalized poly(styrene-*b*-isoprene) system, various block copolymer systems containing a removable block, including poly(styrene-*b*-butadiene),[8,22] poly(styrene-*b*-isoprene),[23,24] poly(styrene-*b*-methyl methacrylate),[25−30] poly(isoprene-*b*-pentameth-

* To whom correspondence should be addressed. Phone: (607) 255-8417. Fax: (607) 255-2365. E-mail: cober@ccmr.cornell.edu.

[†] Department of Materials Science and Engineering, Cornell University.

[‡] Current address: JSR Micro, Inc., Sunnyvale, CA 94089.

[§] Current address: The Institute of Space and Astronautical Science, Kanagawa, Japan.

[∥] Current address: Argonne National Laboratory, Argonne, IL 60439.

[⊥] Cornell High Energy Synchrotron Source (CHESS), Cornell University.

(1) Tolles, W. M. *Nanotechnology* **1996**, *7*, 59.
(2) Lopes, W. A.; Jaeger, H. M. *Nature* **2001**, *414*, 735.
(3) Lee, T.; Yao, N.; Aksay, I. A. *Langmuir* **1997**, *13*, 3866.
(4) Kane, R. S.; Cohen, R. E.; Silbey, R. *Chem. Mater.* **1996**, *8*, 1919.
(5) Temple, K.; Kulbaba, K.; Tower-Billard, K. N.; Manners, I.; Leach, K. A.; Xu, T.; Russell, T. P.; Hawker, C. J. *Adv. Mater.* **2003**, *15*, 297.
(6) Thurn-Albrecht, T.; Schotter, J.; Kästle, G. A.; Emley, N.; Shibauchi, T.; Krusin-Elbaum, L.; Guarini, K.; Black, C. T.; Tuominen, M. T.; Russell, T. P. *Science* **2000**, *290*, 2126.
(7) Lee, J.-S.; Hirao, A.; Nakahama, S. *Macromolecules* **1988**, *21*, 274.
(8) Park, M.; Harrison, C.; Chaikin, P.; Register, R.; Adamson, D. *Science* **1997**, *276*, 1401.
(9) Liu, G.; Ding, J.; Stewart, S. *Angew. Chem., Int. Ed.* **1999**, *38*, 835.
(10) Zalusky, A.; Olayo-Valles, R.; Taylor, C.; Hillmyer, M. *J. Am. Chem. Soc.* **2001**, *123*, 1519.
(11) . Chan, V. Z.-H.; Joffman, J.; Lee, V. Y.; Latrou, H.; Avgeropoulos, A.; Hadjichristidis, N.; Miller, R. D.; Thomas, E. L. *Science* **1999**, *286*, 1716.
(12) Liu, G. *Adv. Mater.* **1997**, *9*, 437.
(13) Raez, J.; Manners, I.; Winnik, M. A. *J. Am. Chem. Soc.* **2002**, 124, 10381.
(14) Cheng, J. Y.; Ross, C. A.; Thomas, E. L.; Smith, H. J.; Vansco, G. J. *Appl. Phys. Lett.* **2002**, *81*, 3657.
(15) Spatz, J. P.; Herzog, T.; Mößmer, S.; Ziemann, P.; Möller, M. *Adv. Mater.* **1999**, *11*, 149;
(16) De Boer, B.; Stalmach, U.; Nijland, H.; Hadziioannou, G. *Adv. Mater.* **2000**, *12*, 1581.
(17) Urbas, A.; Sharp, R.; Fink, Y.; Thomas, E. L.; Xenidou, M.; Fetters, L. J. *Adv. Mater.* **2000**, *12*, 812.
(18) Liu, G.; Ding, J.; Hashimoto, T.; Kimishima, K.; Winnik, F. M.; Nigam, S. *Chem. Mater.* **1999**, *11*, 2233.
(19) Cheng, J. Y.; Ross, C. A.; Chan, V. Z.-H.; Thomas, E. L.; Lammertink, R. G. H.; Vancso, G. J. *Adv. Mater.* **2001**, *13*, 1174.
(20) Asakawa, K.; Hiraoka, T.; Hieda, H.; Sakurai, M.; Kamata, Y.; Naito, K. *J. Photopolym. Sci. Technol.* **2002**, *15*, 465.
(21) Lee, J.-S.; Hirao, A.; Nakahama, S. *Macromolecules* **1988**, *21*, 274.
(22) Harrison, C.; Park, M.; Chaikin, P. M.; Register, R. A.; Adamson, D. H. *J. Vac. Sci. Technol. B* **1998**, *16*, 544.
(23) Park, M.; Chaikin, P. M.; Register, R. A.; Adamson, D. A. *Appl. Phys. Lett.* **2001**, *79*, 257.
(24) Li, R. R.; Dapkus, P. D.; Thompson, M. E.; Jeong, W. G.; Harrison, C.; Chaikin, P. M.; Register, R. A.; Adamson, D. H. *Appl. Phys. Lett.* **2000**, *76*, 1689.
(25) Thurn-Albrecht, T.; DeRouchey, J.; Russell, T. P.; Jaeger, H. M. *Macromolecules* **2000**, *33*, 3250.
(26) Thurn-Albrecht, T.; Steiner, R.; DeRouchey, J.; Stafford, C. M.; Huang, E.; Bal, M.; Tuominen, M.; Hawker, C.; Russell, T. P. *Adv. Mater.* **2000**, *12*, 787.
(27) Mansky, P.; DeRouchey, J.; Russell, T. P.; Mays, J.; Pitsikalis, M.; Morkved, T.; Jaeger, H. *Macromolecules* **1998**, *31*, 4399.
(28) Xu, T.; Hawker, C. J.; Russell, T. P. *Macromolecules* **2003**, *36*, 6178.
(29) Thurn-Albrecht, T.; DeRouchey, J.; Russell, T. P.; Kolb, R.; *Macromolecules* **2002**, *35*, 8106.
(30) Black, C. T.; Guarini, W. *J. Polym. Sci. Part A: Polym. Chem.* **2004**, *42*, 1970.

10.1021/cm0493445 CCC: $27.50
Published on Web 00/00/0000 PAGE EST: 8.1

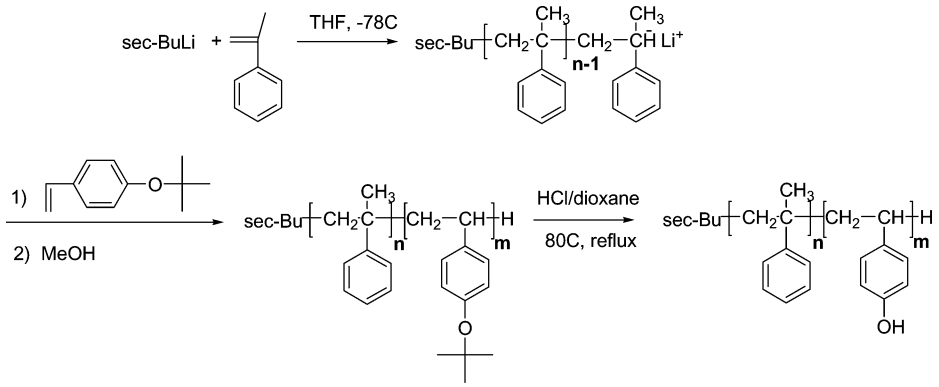

Figure 1. Synthesis of the PαMS-*b*-PHOST block copolymer.

yldisilylstyrene-*b*-isoprene),[11] poly(*tert*-butylacrylate-*b*-2-cinnamoylethyl methacrylate) and related systems,[9,18] poly(styrene-*b*-lactide) and related systems,[10,31,32] and pentadecylphenol-modified poly(styrene-*b*-4-vinylpyridine),[33] have been employed to create ordered monolithic polymers in bulk and thin film states. Additionally, physical means, such as volume contraction triggered by cross-linking[34] and extraction of a blended homopolymer or swelling solvent from block copolymer matrix,[35,36] have also been employed to create nanoporous polymer films.

The optimal utilization of nanoscopic patterns for fabrication requires spatial and orientational control of block copolymer microdomains. In particular, for composition-asymmetric cylindrical block copolymer thin films, an orientation perpendicular to a substrate surface is highly desirable. Three different types of strategies are generally applied for orienting block copolymer thin films: (1) controlling the substrate physical constraints (topography) and thus the film thickness,[37−39] (2) chemical modification of the surface to change the substrate−polymer interactions,[40] and (3) applying external fields (electric, thermal, eutectic solidification, crystallization, and solvent evaporation, etc.) to induce long-range ordering.[6,10,41−47]

The facile fabrication of large-area periodic functional structures or objects with block copolymers is interesting in its own right. However, in many applications, such as multifunctional on-chip bioseparation, simple periodic patterning is insufficient and spatial control of the microdomains is necessary to form integrated multilevel structures.[20] Although there have been reports of obtaining spatial control of functional block copolymer thin film microdomains with e-beam lithography,[48,49] this direct-write patterning process is not time-efficient for high throughput large-area integration of functional devices. Recently we described an approach that combines a conventional "top down" photolithography with a block copolymer-assisted "bottom up" strategy through additive driven phase selective chemistry.[50,51] In this paper, we will describe the domain orientation control and lithographic properties of this system. High-resolution hierarchical structures with the desired orientation can be formed with a wide-range of film thicknesses on different substrates.

Experimental Section

Materials. Chemicals were obtained from Aldrich and used without further purification, unless otherwise noted.

Tetrahydrofuran (THF) was freshly distilled from sodium/benzophenone (deep purple color) under nitrogen and titrated with *sec*-butyllithium before polymerization. Monomers of α-methylstyrene and 4-*tert*-butoxystyrene were successively stirred and distilled with calcium hydride followed by dibutylmagnesium and finally distilled under high vacuum prior to use. Triphenylsulfonium trifluoromethanesulfonate (TPSN) photoacid generator (PAG) was generously provided by JSR Corp. Tetramethoxymethylglycouril (TMMGU) cross-linker was purchase from CYTEC Industries.

Polymer Synthesis. The reactions used for the preparation of poly(α-methylstyrene-*b*-4-hydroxystyrene) (PαMS-*b*-PHOST) are shown in Figure 1.

Block copolymers of poly(α-methylstyrene-*b*-4-*tert*-butoxystyrene) (PαMS-*b*-PtBuOS) were synthesized by sequential living anionic polymerization in 300 mL of THF at −78 °C with 280 μL of 1.3 M *sec*-butyllithium in cyclohexane as the initiator. α-Methylstyrene monomer (5 mL) was polymerized

(31) Zalusky, A. S.; Olayo-Valles, R.; Wolf, J. H.; Hillmyer, M. A. *J. Am. Chem. Soc.* **2002**, *124*, 12761.
(32) Wolf, J. H.; Hillmyer, M. A. *Langmuir* **2003**, *19*, 6553.
(33) Mäki-Ontto, R.; de Moel, K.; de Odorico, W.; Ruokolainen, J.; Stamm, M.; ten Brinke, G.; Ikkala, O. *Adv. Mater.* **2001**, *13*, 117.
(34) Jeong, U.; Ryu, D. Y.; Kim, J. K.; Kim, D. H.; Russell, T. P.; Hawker, C. J. *Adv. Mater.* **2003**, *15*, 1247.
(35) Jeong, U.; Kim, H.-C.; Rodriguez, R. L.; Tsai, I. Y.; Stafford, C. M.; Kim, J. K.; Hawker, C. J.; Thomas, T. P. *Adv. Mater.* **2002**, *14*, 274.
(36) Drzal, P. L.; Halasa, A. F.; Kofinas, P. *Polymer* **2000**, *41*, 4671.
(37) Fasolka, M. J.; Banerjee, P.; Mayes, A. M.; Pickett, G.; Balazs, A. C. *Macromolecules* **2000**, *33*, 5702.
(38) Peters, R. D.; Yang, X. M.; Qiang, Q.; de Pablo, J. J.; Nealey, P. F. *J. Vac. Sci. Technol. B.* **2000**, *18*, 3530.
(39) Segalman R. A.; Hexemer A.; Kramer E. J. *Macromolecules* **2003**, *36*, 6831.
(40) Heier, J.; Genzer, J.; Kramer, E. J.; Bates, F. S.; Krausch, G. *J. Chem. Phys.* **1999**, *111*, 11101.
(41) Keller, A.; Pedemonte, E.; Willmouth, F. M., *Nature* **1970**, *225*, 538.
(42) Hashimoto, T.; Bodycomb, J.; Funaki, Y.; Kimishima, K. *Macromolecules* **1999**, *32*, 2075.
(43) Morkved, T. L.; Lu, M.; Urbas, A. M.; Ehrichs, E. E.; Jaeger, H. M.; Mansky, P.; Russell, T. P. *Science* **1996**, *273*, 931.
(44) De Rosa, C.; Park, C.; Thomas, E. L.; Lotz, B. *Nature* **2000**, *405*, 433.
(45) Kim H. K.; Misner M. J.; Xu T.; Kimura M.; Russell T. P. *Adv. Mater.* **2004**, *16*, 226.
(46) Lin, Z.; Kim, D. H.; Xu, X.; Boosahda, L.; Stone, D.; LaRose, L.; Russell, T. P. *Adv. Mater.* **2002**, *14*, 1373.
(47) Reiter, G.; Caselein, G.; Hoerner, P.; Riess, G.; Blumen, A.; Sommer, J.-U. *Phys. Rev. Lett.* **1999**, *83*, 3844.
(48) Bal, M.; Ursache, A.; Tuominen, M. T.; Goldbach, J. T.; Russell, T. P. *Appl. Phys. Lett.* **2002**, *81*, 3479.
(49) Glass, R.; Arnold, M.; Blümmel, J.; Küller, A.; Möller, M.; Spatz, J. P. *Adv. Funct. Mater.* **2003**, *13*, 569.
(50) Ober, C. K.; Li, M.; Douki, K.; Goto, K.; Li, X. *J. Photopolym. Sci. Technol.*, **2003**, *16*, 347.
(51) Du, P.; Li, M.; Douki, K.; Li, X.; Garcia, C. B. W.; Jain, A.; Smilgies, D.-M.; Fetters, L. J.; Gruner, S. M.; Wiesner, U.; Ober, C. K. *Adv. Mater.* **2004**, *16*, 953.

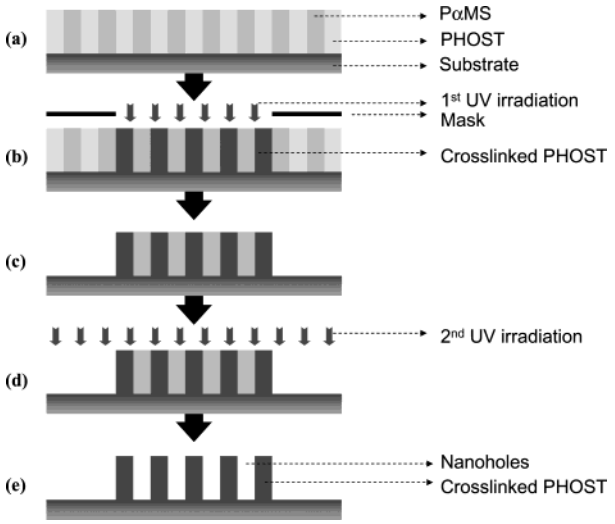

Figure 2. Novel nanofabrication process of obtaining spatially controlled nanopores: (a) spin-coat PαMS-*b*-PHOST/CL/PAG mixture onto a silicon wafer to form vertical cylinders of PαMS in the PHOST matrix, (b) irradiate using a 248 nm stepper with a photomask and bake, (c) develop with a mixed solvent to form micron-sized patterns on top of substrate, (d) irradiate using a 365 nm lamp under vacuum, and (e) form patterns with nanoporous channels.

first for 12 h and an aliquot of poly(α-methylstyryllithium) was isolated for analysis after termination with degassed methanol. 4-*tert*-Butoxystyrene monomer (20 mL) was then introduced into the reactor and the reaction was terminated with degassed methanol after 12 h.

The PαMS-*b*-PtBuOS was converted to poly(α-methylstyrene-*b*-4-hydroxystyrene) (PαMS-*b*-PHOST) by a hydrolysis reaction. Block copolymer (10 g) was first dissolved in 300 mL of dioxane, and 55 mL of 37 wt % hydrochloric acid (10-fold) was added. The mixture was reacted at 80 °C under an atmosphere of nitrogen overnight and then precipitated into 800 mL of water. After neutralization with a 5 wt % NaOH solution to a pH value of 6−7, the resulting polymer was filtered and dried under vacuum at room temperature. The resulting polymer underwent a dissolve−precipitate cycle from 150 mL of THF solution to 500 mL of methanol/water (v/v = 1/1) mixture twice and finally freeze-dried from dioxane.

With a living anionic polymerization procedure similar to the one described above, a homopolymer of poly(α-methylstyrene), with a molecular weight of 2800 g/mol and polydispersity of 1.08, was synthesized and used for the comparison of the thermal properties of the homopolymer with block copolymers.

Nanofabrication Process. Figure 2 shows the novel nanofabrication process that was applied to obtain spatially controlled nanopores. A sample of the PαMS-*b*-PHOST block copolymer was dissolved with a small amount of tetramethoxymethylglycouril (4 wt %) as a cross-linker (CL) and triphenylsulfonium trifluorosulfonate (1.6 wt %) as a photoacid generator (PAG) in propylene glycol methyl ether acetate (PGMEA). Spin-coating of the mixture onto a silicon substrate produced vertically aligned cylinder nanodomains over the entire substrate (Figure 2a). By irradiation through conventional photomasks and subsequent mixed solvent development, a high-resolution photopattern was generated (Figure 2c). Subsequent strong UV irradiation on the developed pattern activates the depolymerization process of the PαMS building block, forming nanosized holes in spatially controlled micron-sized patterns (Figure 2e).

Photoimaging experiments were performed using a Nikon 248 nm stepper (NA = 0.42 and σ = 0.5) equipped with a KrF excimer laser (Cymer CX-2LS) in the Cornell Nanofabrication Facility for the first exposure. Subsequent exposure with a JBA 1000 DUV Resist Cure Ramp (450 mJ/cm^2 at 250 nm) followed by heating (115 °C for 60 s) was used to cross-link the PHOST matrix. A mixed solvent (cyclohexanone/2-propanol = 1/2 in volume) was used as a developer to form the negative-tone photoresist patterns. The thickness of the polymer films was examined with a P-10 profilometer. A second irradiation (70 J/cm^2 at 365 nm) was carried out to remove the PαMS block at 80 °C under high vacuum (~9 × 10^{-5} Torr).

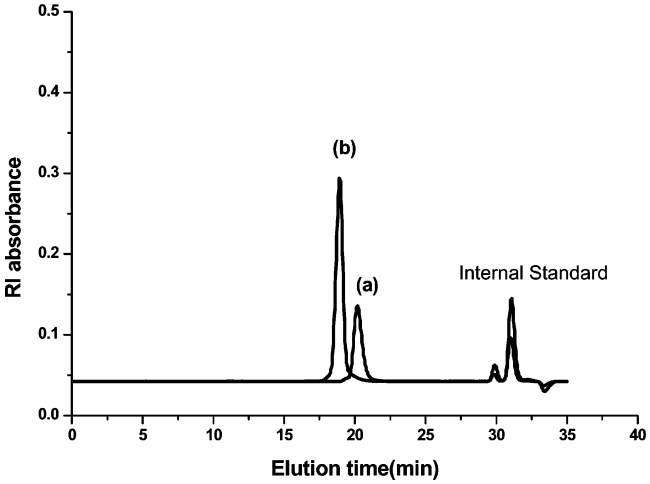

Figure 3. GPC traces of PαMS-*b*-PtBuOS block copolymers: (a) first block poly(α-methylstyrene) (PαMS), M_n = 13 000 g/mol, PDI = 1.09; (b) poly(α-methylstyrene-*b*-4-*tert*-butoxystyrene) (PαMS-*b*-PtBuOS), M_n = 60 500 g/mol, PDI = 1.14.

Characterization. GPC measurements were performed using THF as elution solvent at a flow rate of 1.0 mL/min in a Waters size-exclusion chromatograph (SEC). Narrow polydispersity polystyrene standards were used as calibration standards. ^{1}H NMR spectroscopy was performed on 400 MHz Varian NMR instruments using $CDCl_3$ and DMSO-d_6 as solvents. FT-IR measurements were carried out on a Mattson 2020 Galaxy series instrument. Thermal analysis was carried out on a TA Instruments DSC (DSCQ1000) and a SEIKO thermogravimetric differential thermal analyzer (TGA). Small-angle X-ray scattering (SAXS) and grazing incidence small-angle X-ray scattering (GISAXS) experiments were performed at the Cornell High Energy Synchrotron Source (CHESS) D1 and G1 lines. The X-ray wavelength and intensity and the distance between the sample and CCD detector were easily adjusted according to the requirements of each experiment. The collected GISAXS 2-D images were processed with the FIT2D program. The surface structures of the polymer thin film on silicon substrates were examined with AFM using a Veeco Dimension 3100 scanning probe microscope operated in tapping mode with Olympus tapping mode etched silicon probes (resonant frequency = 300 kHz, force constant = 42 N/m, tip radius of curvature = 10 nm; all values nominal) under ambient conditions.

Results and Discussion

Synthesis and Characterization of PαMS-*b*-PHOST Block Copolymers. A block copolymer, PαMS-*b*-PHOST, with a total molecular weight of 45 400 g/mol and PαMS weight ratio of 28%, was designed and prepared by living anionic polymerization and subsequent hydrolytic deprotection (the GPC trace in Figure 3 shows the protected PαMS-*b*-PtBuOS block copolymer obtained after polymerization, with narrow molecular weight distribution: PDI = 1.14). Living anionic polymerization of the α-methylstyrene monomer[52,53] and protected hydroxystyrene monomer[54,55] are well-docu-

(52) Morton, M. *Anionic Polymerization: Principles and Practice*; Academic Press: New York, 1983; p 18.
(53) Burger, D. E.; Bruss, D. B. *J. Polym. Sci., Part A: Polym. Chem.* **1963**, *12*, 1927.

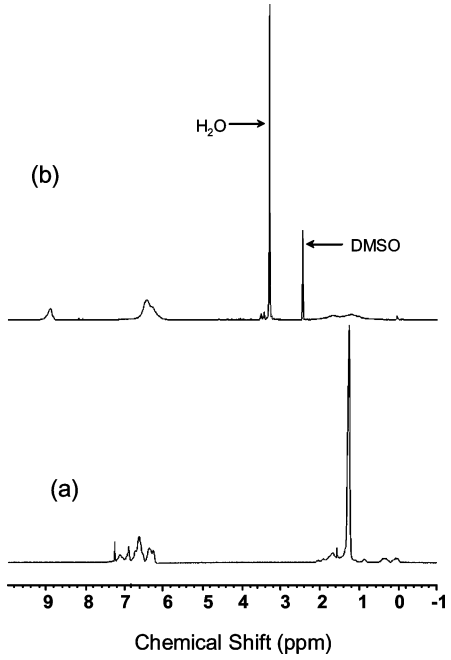

Figure 4. ^{1}H NMR spectrum (a) before hydrolysis, PαMS-*b*-PtBuOS ($CDCl_3$), and (b) after hydrolysis (DMSO-d_6), PαMS-*b*-PHOST.

mented, although this diblock copolymer system has not been previously investigated. To obtain a monodisperse PHOST block, it is necessary to protect the hydroxy group before polymerization to avoid the termination of the living chain end. Various protecting groups, including *tert*-butyl ether[54] and *tert*-butyldimethylsilyl group,[55] have been used for hydroxyl group protection, and successful living character has been achieved in the anionic polymerization process. In this case, *tert*-butyl ether protected monomer was used because of its ready availability and ease of hydrolysis.

The chemical composition of the block copolymer was determined by ^{1}H NMR spectroscopy (Figure 4). A chemical shift of 1.2 ppm corresponds to the *tert*-butyl group of PαMS-*b*-PtBuOS block copolymer (in $CDCl_3$). The spectrum of PαMS-*b*-PHOST (in DMSO-d_6) shows a peak at 8.8 ppm, which corresponds to the hydroxyl group after the deprotection reaction. No signal due to the *tert*-butyl group remains, and only polymer backbone protons appear in the chemical shift region of 1−2 ppm. The FTIR spectrum of PαMS-*b*-PHOST (Figure 5) shows a peak at 3380 cm^{-1}, which indicates the presence of the OH group after deprotection. The disappearance of a peak at 1132 cm^{-1} [56] indicates complete removal of the *tert*-butyl ether groups during hydrolysis.

Thermal analysis was carried out on both homopolymer PαMS and block copolymers. The T_g of the PαMS homopolymer was found to be 144 °C, while PαMS-*b*-PtBuOS showed the T_g of the PαMS block at 133 °C and the T_g of PtBuOS was indistinguishable, possibly convoluted with the PαMS thermal transition. The hydrolyzed PαMS-*b*-PHOST block copolymer also showed

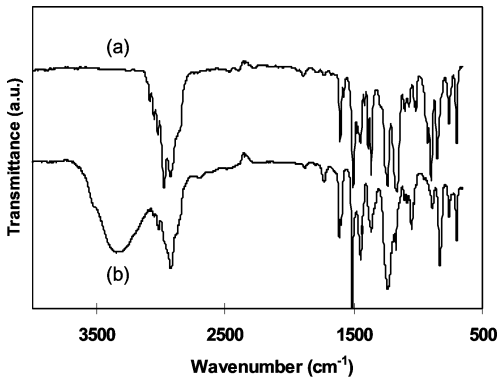

Figure 5. FTIR spectra of (a) PαMS-*b*-PtBuOS and (b) PαMS-*b*-PHOST.

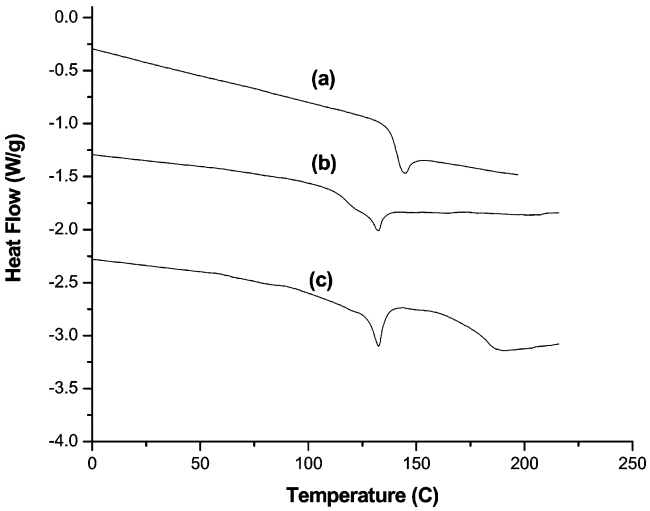

Figure 6. DSC analysis of (a) poly(α-methylstyrene), (b) poly(α-methylstyrene-*b*-4-*tert*-butoxystyrene), and (c) poly(α-methylstyrene-*b*-4-hydroxystyrene).

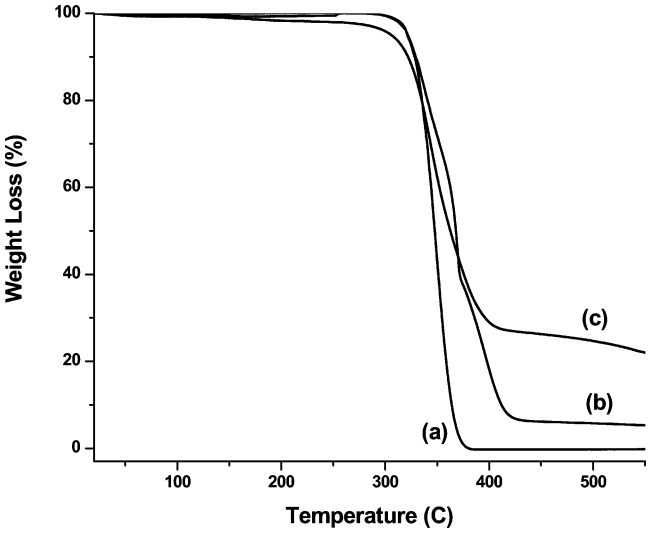

Figure 7. TGA analysis of (a) poly(α-methylstyrene), (b) poly(α-methylstyrene-*b*-4-*tert*-butoxystyrene), and (c) poly(α-methylstyrene-*b*-4-hydroxystyrene).

the T_g of PαMS at 130 °C as well as the T_g of PHOST at around 180 °C (Figure 6). Thermal gravimetric analysis of homo-PαMS, PαMS-*b*-PtBuOS, and PαMS-*b*-PHOST were performed (Figure 7). No significant weight loss was found for any of the polymer systems below 300 °C.

(54) Se, K.; Miyawaki, K.; Hirahara, K.; Takano, A.; Fujimoto, T. *J. Polym. Sci., Part A: Polym. Chem.* **1998**, *36*, 3021.
(55) Ito, H.; Knebelkamp, A.; Lundmark, S. B.; Nguyen, C. V.; Hinsberg, W. D. *J. Polym. Sci., Part A: Polym. Chem.* **2000**, *38*, 2415.
(56) Colthup, N. B. *J. Opt. Soc. Am.* **1950**, *40*, 397.

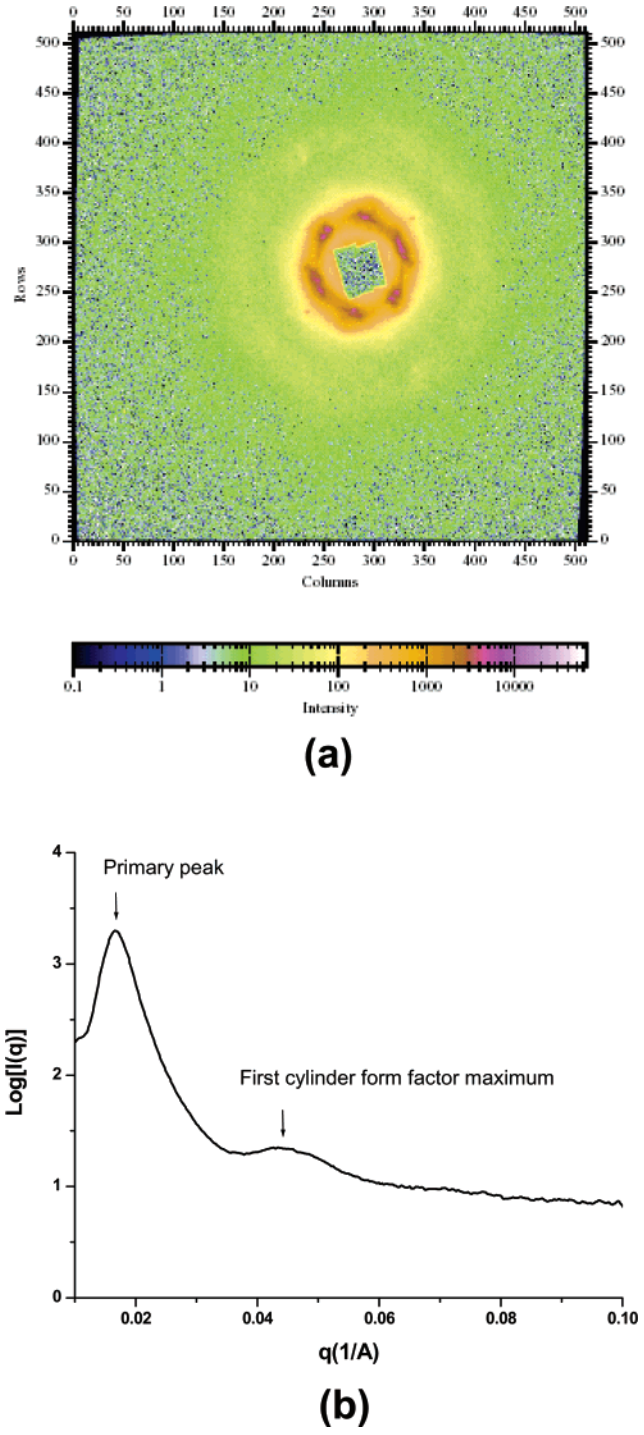

Figure 8. SAXS pattern of a bulk sample of PαMS-*b*-PHOST (cast from THF). A hexagonal cylinder microstructure of the sample is obtained. The primary peak and the first cylinder form factor maximum were clearly observed. Intercylinder distance was identified to be 38 nm.

Figure 8 shows the small-angle X-ray scattering (SAXS) patterns of a bulk sample of the PαMS-*b*-PtBuOS block copolymer cast from THF and annealed at 200 °C for 2 days, which indicates a hexagonal cylinder morphology. The primary peak and the first cylinder form factor maximum were clearly observed, while the lack of long range order can be rationalized as due to the relatively low annealing temperature used compared to the high T_g of the PHOST phase. This temperature was necessitated by the low thermal stability of the block copolymer (thermal cross-linking of PHOST and the onset of PαMS decomposition). The intercylinder distance was determined to be 38 nm.

Deprotection of the PαMS Block. In this patternable nanoporous system, PαMS was designed to form the cylinder minor phase, which can be easily removed from the PHOST matrix because of its low ceiling temperature (61 °C).[57] However, simple heating does not initiate the depolymerization process, as shown by thermogravimetric analysis (Figure 7). No significant thermal loss was observed below 300 °C with a heating rate of 10 °C/min. One possible explanation for this behavior is that the polymer's ceiling temperature is defined by the equilibrium state of polymerization with depolymerization processes, which requires the coexistence of the active polymer chain ends with monomers.[57] Thus, special treatment such as UV irradiation is necessary to generate the needed unstable radicals, which then trigger the step-by-step unzipping of polymer chains above the ceiling temperature. To get complete depolymerization of the PαMS block, high vacuum conditions are also critical to remove the liberated monomers and thus drive the polymerization−depolymerization equilibrium toward the monomer state. By manipulating processing conditions, it was determined that PαMS can be depolymerized efficiently under strong UV irradiation (70 J/cm^2) with high vacuum treatment when held at 80 °C.

Lithographic Characteristics of the PHOST Block. In this patternable block copolymer system, PHOST was designed as a negative-tone photoresist[58] when TMMGU (4 wt %) was used as cross-linker[59,60] and TPSN (1.6 wt %) as photoacid generator. TMMGU and TPSN were selected primarily due to their thermal stability up to 200 °C.[54] Exposure to low levels of 248 nm UV radiation triggers generation of acid by the PAG, which induces an electrophilic attack at the oxygen atom of the methoxy group of the TMMGU. Elimination of methanol in the intermediate leads to the formation of a carbocation, which undergoes further electrophilic attack at the oxygen atom of the phenolic hydroxyl group to efficiently cross-link the PHOST block (Figure 9).[60] Regardless of the local distribution of the reactants, this cross-linking chemistry only takes place in the PHOST matrix phase and thus generates the solubility switch necessary for lithographic patterning.

AFM measurements were performed before and after every processing stage and they show that the cylindrical morphology is maintained throughout the entire process. Figure 10a shows an AFM image obtained from the block copolymer after spin coating the mixture from PGMEA on a silicon wafer. It was found that even in the presence of small amounts of additives, cylinders with a diameter of 25 nm are detected on top of the substrate. An AFM image obtained after weak flood irradiation and heating to cross-link the matrix is shown in Figure 10b, indicating that the cylinders remain

(57) Brandrup, J.; Immergut, E. H.; Grulke, E. A. *Polymer Handbook*, 4th ed.; Wiley-Interscience: New York, 1999; II, p 394.
(58) Ito, H. *J. Polym. Sci. Part A: Polym. Chem.* **2003**, *41*, 3863.
(59) Lin, Q.; Katnani, A.; Willson, C. G. *Proc. SPIE-Int. Soc. Opt. Eng.* **1997**, *3049*, 974.
(60) Röschert, H.; Dammel, R.; Eckes, C.; Kamiya, K.; Meier, W.; Przybilla, K.-J.; Spiess, W.; Pawlowski, G. *Proc. SPIE-Int. Soc. Opt. Eng.* **1992**, *1672*, 157.

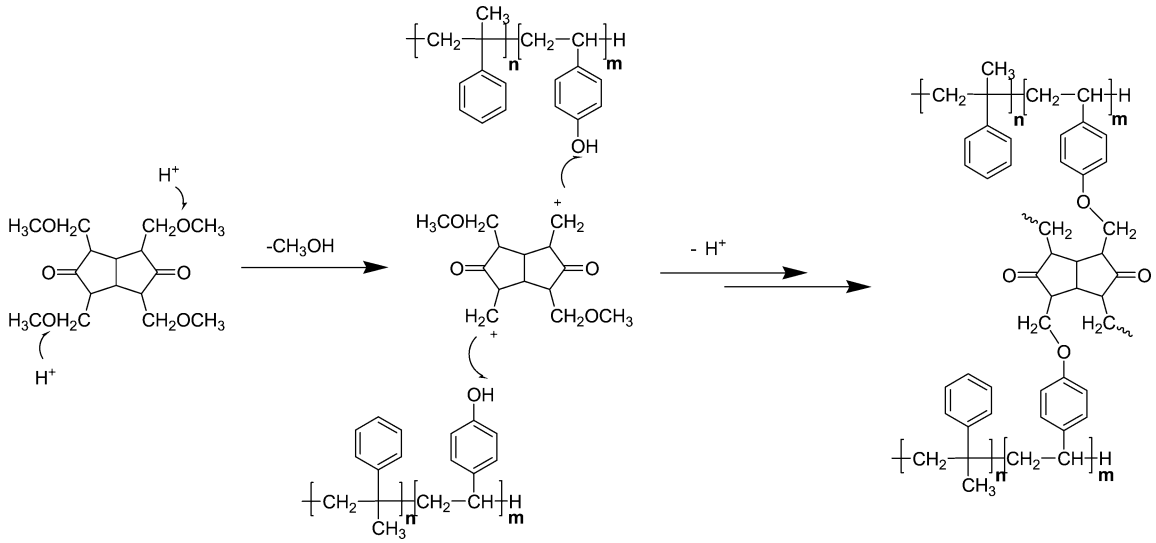

Figure 9. Proposed cross-linking mechanism of PαMS-*b*-PHOST with TMMGU (ref 60).

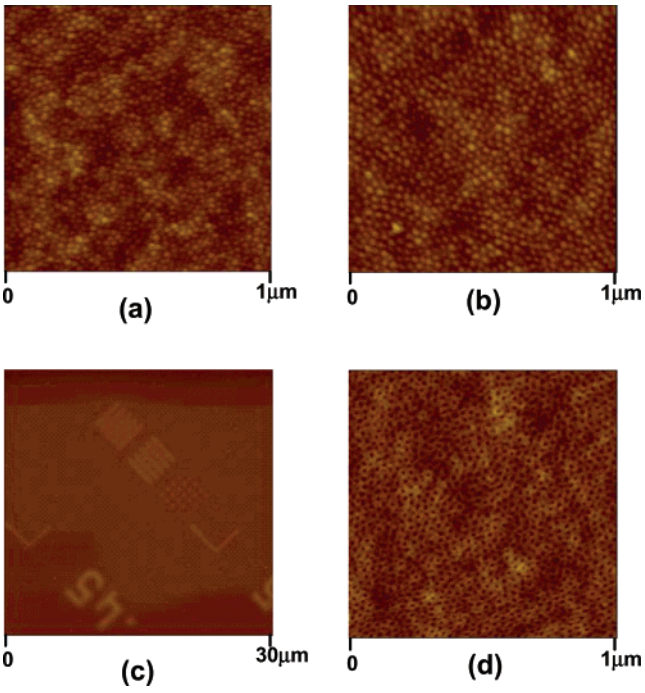

Figure 10. AFM height images obtained from thin films of PαMS-*b*-PHOST on a silicon wafer: (a) after spin coating from PGMEA without annealing; (b) after development, the microstructure and its orientation were retained; (c) patterns with feature size as small as 450 nm were obtained after development; (d) further UV irradiation generated nanometer-sized pores on the patterned region.

intact. A range of solvents was examined to develop the films after exposure with a 248 nm stepper. High-resolution photopatterns were generated with resolution as small as 450 nm, as shown in Figure 10c. A second irradiation step under vacuum produced uniformly sized holes, having a diameter of 18 nm in the patterned area without any collapse, as shown in Figure 10d.

Influence of Film Thickness. Different thicknesses of the polymer membranes have been studied in order to evaluate their lithographic properties. Two films of different thickness were used as representative examples: 72 and 152 nm (after spin coating). In the case of the 72 nm thin film (Figure 11A), the first irradiation (65 mJ/cm^2) generated photopatterns with a resolution of 1.5 and 2.0 μm, as shown in Figure 11a. Because of the removal of PαMS materials, the film thickness after development was measured to be 39 nm. This thickness loss can be rationalized as the effect of covalent coupling of adjacent polymer chains and thus densification during the cross-linking of the PHOST phase. A similar process has been fully described by Russell and coworkers in a UV-cross-linked PS-*b*-PMMA system.[34] The second mild irradiation created nanosized pores in the photopatterns, as shown in Figure 11b−d. Although the pores do not appear to be very uniform due to the top-rounding of the photopatterns, it is believed that optimization of the process to generate rectangular photopatterns can improve uniformity. In the case of the 152 nm film (Figure 11B), refined pores were obtained on the photopatterns. A 152 nm thin film was developed after the first irradiation (21 mJ/cm^2) and resulted in a film with a thickness of 127 nm. The second irradiation produced uniform pores in the high-resolution photopatterns, as shown in Figure 11e−g. As shown there, the photopatterns possess very refined surface structure.

GISAXS Study of the Orientation of the Thin Film Structures. The control over polymer domain orientation is critical for the optimum application of nanoporous block copolymer thin films. However, the control over orientation and lateral order of microdomains in thin films remains a challenge. In this study, PαMS-*b*-PHOST copolymer forms the cylindrical microdomains, which preferentially align vertically on the substrate directly after spin-coating. This unique property has been observed in some other block copolymer systems [5,45,46,61−65] and was rationalized as being the result of entropic contribution[65] or the zone-refinement effect[5,45] during the nonequilibrium fast evaporation of the solvent in the spin-coating process.

(61) Fukunaga, K.; Elbs, H.; Magerle, R.; Krausch, G. *Macromolecules* **2000**, *33*, 947.
(62) Kim, G.; Libera, M. *Macromolecules* **1998**, *31*, 2569.
(63) Mansky, P.; Chaikin, P.; Thomas, E. L. *J. Mater. Sci.* **1995**, *30*, 1987.
(64) Turturro, A.; Gattiglia, E.; Vacca, P.; Viola, G. T. *Polymer* **1995**, *36*, 3987.
(65) Busch, P.; Posselt, D.; Smilgies, D.-M.; Rheinländer, B.; Kremer, F.; Papadakis, C. M. *Macromolecules* **2003**, *36*, 8717.

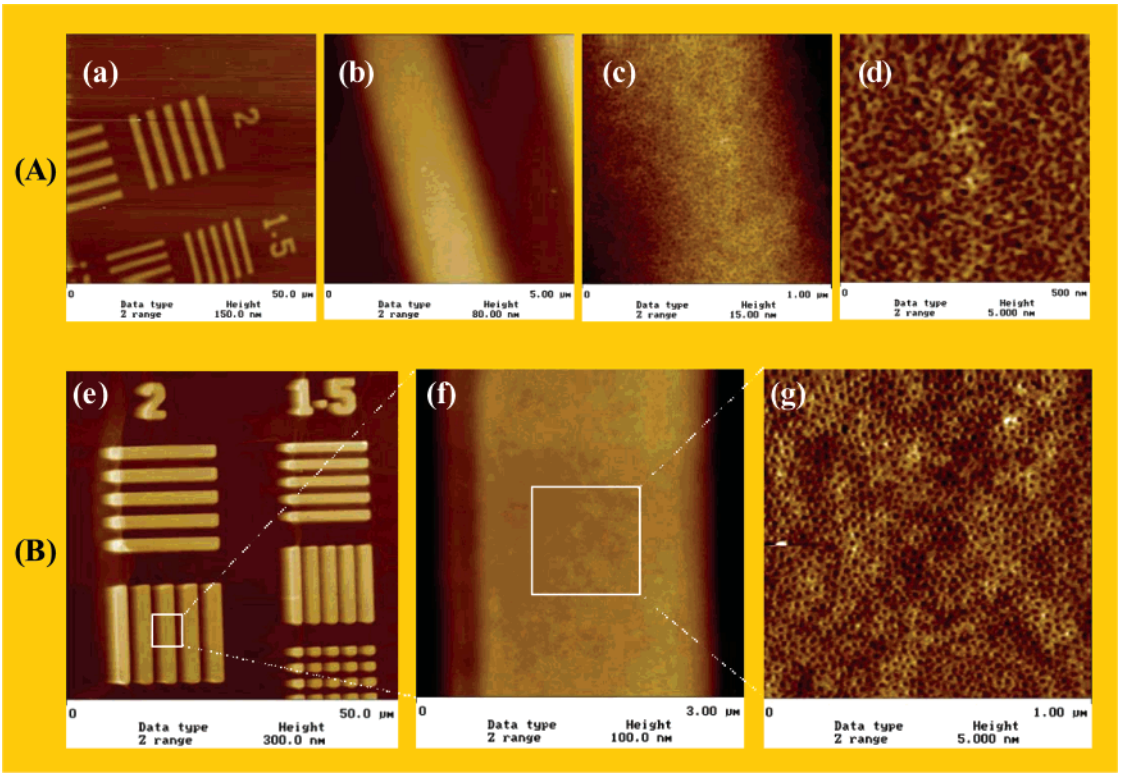

Figure 11. AFM height images obtained from thin films of PαMS-*b*-PHOST on a silicon wafer after removal of PαMS materials from photopatterned polymer matrix created by a 248 nm stepper. (A) Film thickness is 39 nm, with (a) 2 and 1.5 μm lines shown. (b) A magnification of a 2 μm line. (c) A further magnification of the line. (d) A further magnification of the line. (B) Film thickness is 127 nm, with (e) 2 and 1.5 μm lines and dots shown. (f) A magnification of a 2 μm line. (g) A further magnification of the line.

To test the internal thin film structure on macroscopic length scales and to demonstrate that the AFM images of Figure 9 are representative over the whole thickness of the film, we employed grazing incidence small-angle X-ray scattering (GISAXS) to probe the orientation of the nanostructures in the thin films. The intensity in a GISAXS image results from the electron density difference between the two phases. Since both blocks in the PαMS-*b*-PHOST system are hydrocarbon chains, the electron density difference between the blocks is much smaller than that between polymer and air. Therefore, this technique proves useful for confirming nanochannel creation in a thin film by monitoring the scattering intensity difference before and after removal of the PαMS block.

Figure 12a shows a two-dimensional GISAXS image taken from the thin film (152 nm in thickness) before the UV removal of the PαMS block. The vertical streaks in the GISAXS pattern indicate that the PαMS cylinders orient perpendicular to the substrate[66] with an intercylinder distance determined to be 33.5 nm. With the complete removal under vacuum of PαMS during the second UV irradiation, vertical streaks with a much stronger scattering intensity appear at the same q_x value in the GISAXS image (Figure 12b). This indicates that there is a much larger density contrast after treatment that we ascribe to hollow nanochannels being generated in the polymer film. Moreover, the persistence of the vertical streaks shows that the nanochannels are formed without any significant collapse of the matrix polymer block after the removal of PαMS.

To investigate the thickness and substrate effects on the orientation of the spin-coated PαMS-*b*-PHOST films, GISAXS measurement were also taken on a thicker film (~1 μm), as well as a film spin-coated on a poly(acrylic acid) substrate. In the thick film case, GISAXS images were taken at incident angles of $0.25\alpha_c$ (Figure 13a) and $1.5\alpha_c$ (Figure 13b). Both show the streaks in the scattering intensity characteristic of vertical cylinders, where α_c is the critical angle of the polymer film of 0.135°. At $0.25\alpha_c$ the X-ray penetration depth is only 10 nm, from which we discern that the film is ordered at the air−polymer interface. At $1.5\alpha_c$ the X-ray penetration depth is about 15 μm and hence the X-ray beam is scattered from the full thickness of the polymer film. The fact that the scattering pattern is still streak-like shows that the cylinders are oriented vertical to the substrate throughout the film. Had there been a 3D microstructure in the interior of the film, as typical for bulk samples, we would expect to see a ringlike scattering feature in addition to the streaks. Similarly, we also found that the vertical streak remains in the GISAXS image of the block copolymer thin film that was spin-coated on the PAA substrate, which indicates that the perpendicular cylindrical orientation of the block copolymer can be induced over a wide range of thicknesses on different substrates through the simple spin-coating process.

Conclusion

In summary, a novel patternable block copolymer PαMS-*b*-PHOST was designed and synthesized. The PHOST block was investigated as a negative -tone

(66) Smilgies, D.-M.; Busch, P.; Posselt, D.; Papadakis, C. M. *Synchorotron Radiat. News* **2002**, *15*, 35.

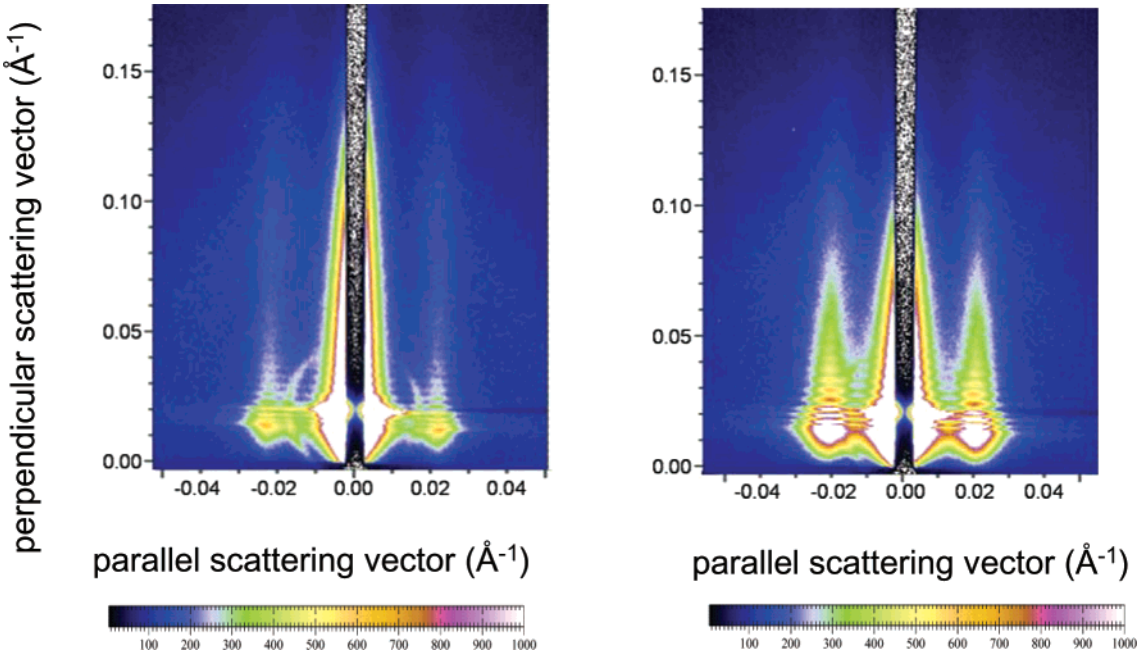

Figure 12. GISAXS images obtained from a thin film of PαMS-*b*-PHOST (152 nm in thickness) on a silicon wafer. X-rays of wavelength $\lambda = 0.155$ nm incident at 0.2075° to the film surface were used. (a) Before removal of PαMS block. The vertical streaks indicate that the cylinders standing up on the silicon substrate throughout the film. (b) After removal of PαMS block. The dramatic increase of the scattering contrast of the streaks indicates the nanoporous nature of the thin film.

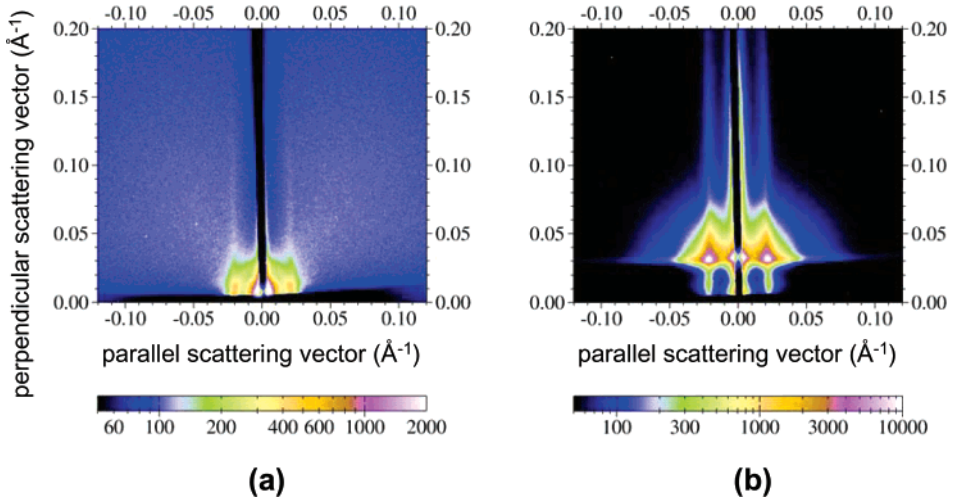

Figure 13. GISAXS images of a 1 μm thick diblock copolymer film of PαMS-*b*-PHOST. The vertical streaks are characteristic of lateral ordering of the cylinders in the film. The intense scattering in the incident plane (center of the images) is blocked by a rodlike beamstop. For panel a, the incident angle was chosen at a quarter of the polymer critical angle, limiting the X-ray penetration depth to about 10 nm. The streaklike scattering indicates that the cylinders are oriented perpendicular to the substrate in the region near the top surface of the polymer film. In panel b, the incident angle was 1.5 times the critical angle, yielding a full penetration of the film by the X-ray beam. The streaklike scattering shows that the cylinders are oriented perpendicular to the substrate throughout the full thickness of the polymer film.

photoresist, while the PαMS block was studied as a degradable unit to form a nanoporous medium. With a simple spin-coating process, this polymer self-assembled to generate PαMS cylinders oriented normal to the substrate in a PHOST matrix over a wide range of film thicknesses. This orientation was confirmed using GISAXS for both as-deposited films and for films with the minority PαMS phase removed. Through a combination of advanced photolithographic and nanofabrication processes, spatial control of the nanopores with desired orientation was achieved in a user-friendly manner. These high-resolution hierarchical structures can function as nanodevices themselves, and for example, they are being explored as porous bioseparation media for use in future integrated bioanalysis systems. Furthermore, they can also serve as patterned templates or scaffolds for the fabrication of various types of multifunctional nanomaterials.

Acknowledgment. This work was supported by the Nanobiotechnology Center (NBTC), an STC Program of the National Science Foundation under Agreement No. ECS-9876771. Partial support from the NSF-funded Cornell NIRT (ECS-0103297-NIRT) and grant NSF DMR-0208825 is also acknowledged. We thank CHESS and Cornell Nanofabrication Center for using their

facilities. CHESS is a national user facility supported by NSF/NIH/NIGMS award DMR 0225180. We also thank Prof. Uli Wiesner and his group for ongoing collaborations in the area of phase specific chemistry of block copolymers. Finally, we would like to thank both Prof. Sol M. Gruner and Prof. Lewis J. Fetters for useful discussions and acknowledge the use of the facilities in the Gruner labs.

CM0493445